



Published in final edited form as:

*Opt Lett.* 2009 September 1; 34(17): 2566–2568.

## Transillumination fluorescence imaging in mice using biocompatible upconverting nanoparticles

Claudio Vinegoni<sup>1,\*†</sup>, Daniel Razansky<sup>2,†</sup>, Scott A. Hilderbrand<sup>1</sup>, Fangwei Shao<sup>1</sup>, Vasilis Ntziachristos<sup>2</sup>, and Ralph Weissleder<sup>1</sup>

<sup>1</sup>Center for Systems Biology, Massachusetts General Hospital, Harvard Medical School, 185 Cambridge Street, Boston, Massachusetts 02114, USA

<sup>2</sup>Institute for Biological and Medical Imaging (IBMI), Technical University of Munich and Helmholtz Center Munich, Ingolstaedter Landstrasse 1, 85764 Neuherberg, Germany

### Abstract

We report on a systematic study of upconverting fluorescence signal generation within turbid phantoms and real tissues. An accurate three-point Green's function, describing the forward model of photon propagation, is established and experimentally validated. We further demonstrate, for the first time to our knowledge, autofluorescence-free transillumination imaging of mice that have received biocompatible upconverting nanoparticles. The method holds great promise for artifact-free whole-body visualization of optical molecular probes.

A large number of modalities for small-animal *in vivo* fluorescence imaging have emerged in recent years. Of particular interest is the visualization of fluorescent probes and proteins used to gain insight into molecular targets and physiology. Volumetric optical-imaging techniques, such as transillumination planar fluorescence imaging [1] and fluorescence molecular tomography (FMT) [2], have already proven to be extremely useful in detecting fluorescence signal deep in turbid tissue. Furthermore, FMT can now provide three-dimensional tomographic maps of fluorescence activity through the entire body of small animals *in vivo*. While both techniques provide low spatial resolution, they are noninvasive and have been exploited for *in vivo* imaging of proteases, angiogenesis, and tumor receptors, introducing new venues in biological research [3]. Both FMT and transillumination planar imaging methods are performed by illuminating the sample with a beam of light (excitation wavelength) and obtaining images from fluorescence molecular agents in transillumination mode using a CCD camera combined with appropriate imaging optics [4]. However, the presence of nonspecific induced autofluorescence due to intrinsic tissue fluorochromes can drastically limit the sensitivity and contrast in the images. Since most dyes and other markers like quantum dots emit fluorescence in the Stokes part of their emission spectra, different strategies have been developed in order to minimize this opposing effect primarily by using different subtraction schemes [4]. Multispectral approaches have also been considered for simple photographic (epi-illumination) imaging, but their implementation to volumetric imaging is significantly more challenging. To reduce the effects of autofluorescence, we consider in this Letter a fundamentally different approach based on the use of a new class of upconverting nanoparticles (UNP) [5]. While conventional fluorescence is based on single-photon excitation, the upconversion fluorescence principle is based on the conversion of two or more photons of low energy in the near IR into one photon at higher energy. Differently from two-photon

\*Corresponding author: cvinegoni@mgh.harvard.edu.

†These authors contributed equally to this work.

fluorescence, the absorption of the low-energy photons does not involve a virtual level, and the cross section is therefore orders of magnitude higher. This permits the use of cheaper cw lasers, in contrast to two-photon fluorescence, where pulsed lasers, such as Ti:sapphire, are commonly used. Owing to the lack of tissue autofluorescence in the anti-Stokes part of the spectrum, UNPs are particularly well suited for background-free signal collection while at the same time allowing us to image deeper into tissue. We present a systematic study of biocompatible UNPs in media closely resembling that encountered *in vivo*. We further suggest description of the upconversion using a three-point Green's function for upconversion and provide the necessary quantitative experimental validation in tissue-type phantoms. Finally, results of autofluorescence-free transillumination imaging of a mouse implanted with fluorescent tubes postmortem are presented. The UNPs used here are yttrium oxide ( $Y_2O_3$ ) nanoparticles doped with erbium and ytterbium [5]. These nanoparticles present very strong upconversion emission at 660 nm after excitation at 980 nm [5]. While most methods to produce UNP give rise to uncoated or hydrophobic-molecules-coated particles that either aggregate strongly or do not suspend in water, our particles are first coated with polyacrylic acid and coupled to 2000 MW mPEG-NH<sub>2</sub> polyethylene glycol polymers. This protective shell allows the polymers to obtain long-term aqueous stability, making them suitable for *in vivo* imaging application [5]. We first characterized the UNP by studying the dependence of the upconversion fluorescence as a function of the pump power to verify that the process is nonlinear. In Figs. 1(a) and 1(b) we plot the emission fluorescence as a function of excitation power for both a regular near-IR fluorescence dye (Cy5.5, open circles) and the UNP (squares) where the thin lines represent the best fit. The data clearly show that, while for Cy5.5 we have a linear dependence for the emitted light in the excitation power as expected, the emission from the UNP originates from a two-photon process. To understand the propagation of the upconverted photons in diffusive media and to exploit them for reconstruction, the Green's function describing the forward light-propagation model needs to be determined. In fact, its accurate knowledge will allow one to conveniently employ inversion methods commonly used for fluorescence molecular tomography and to tomographically reconstruct and quantify UNP distribution within tissue. Images were therefore collected with a custom-built imaging scanner for planar imaging. The system consists of a small-animal imaging chamber with parallel plates, an excitation laser, a galvo-controlled optical scanner with focusing optics, an imaging telecentric lens, and a detection camera. Light from the laser diodes was filtered through appropriate bandpass filters (FWHM 10 nm) and subsequently focused onto a specific spot of one plate of the imaging chamber. Emitted fluorescence signal was filtered with a long-pass or short-pass filter (Cy5.5 or UNP, respectively) combined with appropriate bandpass filters (FWHM 10 nm) while the images were collected in transillumination mode with a highly sensitive CCD camera. The mouse transillumination images were acquired as the sum of the transmitted diffused light for different illumination spots [crosses on the white-light image of Fig. 2(a)]. The chamber was water sealed and filled with an optical matching fluid with tissue-like absorbing and scattering properties to remove straight light components and avoid CCD pixel saturation. For this study, the source–detector distance was fixed at 12 mm.

In the first set of experiments, aimed at determining the three-point Green's function, the imaging chamber was filled with a 12-mm-wide slab prepared from a solution of intralipid and India ink, attaining a reduced scattering coefficient of  $\mu'_s=20\text{ cm}^{-1}$  and an absorption coefficient  $\mu_a=1\text{ cm}^{-1}$  at 680 nm, validating the use of the diffusion approximation. A thin glass tube (inner diameter of 0.5 mm), containing small volume of either UNP or far-red fluorescent dye (Cy5.5; excitation, 675 nm; emission, 712 nm), was submerged into the slab and translated through the 12 mm of its width. Cy5.5 was chosen because it emits in a near-IR region near the UNP emission range and because it is often used for *in vivo* imaging. For UNP detection, the slab was illuminated by a point laser source (focal diameter, 0.5 mm) at a wavelength of 980 nm (power, 120 mW), while a 680 nm laser was used for Cy5.5. Integration times for UNP and

Cy5.5 measurements were 10 and 1 s, respectively. Results of the experiments are presented in Fig. 1(c), where signal intensities, integrated over the entire CCD image, are plotted against the distance of the tube from the illuminated surface. The signal detected from the UNP dropped rapidly as the tube moved away from the light source into the turbid medium.

To provide the explicit governing equations for UNP excitation and detection in a turbid medium, we have assumed their excitation efficiency to be proportional to local light intensity to the power of  $n$ , i.e., for point-source excitation,

$$G_{\text{exc}}^{\text{NP}}(\vec{r}_s, \vec{r}) = \left( \frac{e^{-k_1|\vec{r}_s - \vec{r}|}}{|\vec{r}_s - \vec{r}|} \right)^n = \frac{e^{-nk_1|\vec{r}_s - \vec{r}|}}{|\vec{r}_s - \vec{r}|^n}, \quad (1)$$

where  $k_1 = \sqrt{3\mu_a(\mu_a + \mu'_s)}$  is the diffuse photon propagation wave number at 980 nm,  $\vec{r}_s$  is the source position, and  $\vec{r}$  is the UNP position. The emitted radiation undergoes the usual light diffusion process, described via

$$G_{\text{fluo}}^{\text{NP}}(\vec{r}, \vec{r}_d) = \frac{e^{-k_2|\vec{r} - \vec{r}_d|}}{|\vec{r} - \vec{r}_d|}, \quad (2)$$

where  $k_2$  is the corresponding wave number at 680 nm and  $\vec{r}_d$  is the detector position on the opposite side of the slab. The integrated signal detected by the CCD can be therefore expressed via

$$U(\vec{r}_s, \vec{r}) \sim \int G_{\text{exc}}^{\text{NP}}(\vec{r}_s, \vec{r}) A(\vec{r}) G_{\text{fluo}}^{\text{NP}}(\vec{r}, \vec{r}_d) dS, \quad (3)$$

where  $dS$  denotes integration over the CCD detection plane and  $A(\vec{r})$  is the local UNP concentration. For Cy5.5, we assumed excitation at 680 nm with Green's function as in Eq. (1) with  $n=1$ . The emission and integration were as in Eq. (2) and expression (3), respectively.

The measured data fit well the theoretical predictions in Eqs. (1) and (2) and expression (3) for  $n=2.3$ , as shown in Fig. 1(c). Clearly, while moving the tube filled with the fluorescent dye away from the source results only in a slight decrease of the detected intensity, the transillumination signal due to the UNP drops drastically by 2 orders of magnitude once the tube is translated for several millimeters into the slab. To test the performance of the particles for potential small-animal imaging application, we also acquired transillumination images of animals with glass capillary tubes inserted in their esophagus, as shown in Fig. 2. A mouse is held between the two glass plates of the imaging chamber and slightly compressed to a thickness of 12 mm. Figure 2(a) shows the white-light epi-illumination image with the associated illumination geometry (crosses). The transillumination images are all averaged over all 36 sources and are taken for the capillary tube filled with 100 nM of Cy5.5 and 40 nM of UNPs in buffered solution, while the excitation occurs at 680 nm (upper row) and 980 nm (lower row), respectively. In all the transillumination images the signal is overlaid on top of the corresponding white image after color mapping. Figure 2(b) shows the intrinsic signal for both excitation wavelengths, while Fig. 2(d) shows the fluorescence signal due to excitation of the Cy5.5 (upper row) and the UNP (lower row), respectively. Autofluorescence contribution in the mouse is totally absent when excitation occurs at 980 nm [Fig. 2(c)].

Apparently, in contrast to the conventional Cy5.5 fluorescence imaging [Fig. 2(d)], upconversion resulted in few background artifacts and accurately resolved the glass tube filled with the UNP.

In conclusion, we show the feasibility of using biocompatible upconverting nanoparticles for mice imaging. Autofluorescence-free transillumination imaging in a mouse was demonstrated, while the data obtained for UNPs were compared with results obtained using a near-IR dye commonly used in fluorescence molecular tomography. Moreover, an accurate experimental and theoretical description of the three-point Green's function was provided and experimentally validated. This allows one to construct an accurate forward model of the upconverted photons propagation, an important step for solving the inverse problem and for the UNP exploitation for fluorescence tomography. Free-space 360 tomography should help in reducing signal from nonspecific up-taken UNPs present in the first tissue layers. Overall, we envision that the UNPs could be successfully used for whole-body fluorescence imaging studies, providing background-free tomographic reconstructions while simultaneously improving image quality and contrast.

## Acknowledgments

C. Vinegoni acknowledges support from National Institutes of Health (NIH) (grant 1-RO1-EB006432).

## References

1. Zacharakis G, Shih H, Ripoll J, Weissleder R, Ntziachristos V. *Mol Imaging* 2006;5:153. [PubMed: 16954030]
2. Zacharakis G, Kambara H, Shih H, Ripoll J, Grimm J, Saekl Y, Weissleder R, Ntziachristos V. *Proc Natl Acad Sci USA* 2005;102:18252. [PubMed: 16344470]
3. Ntziachristos V, Ripoll J, Wang L, Weissleder R. *Nat Biotechnol* 2005;23:313. [PubMed: 15765087]
4. Soubret A, Ntziachristos V. *Phys Med Biol* 2006;51:3983. [PubMed: 16885619]
5. Hilderbrand SA, Shao F, Salthouse C, Mahmood U, Weissleder R. *Chem Commun* 2009;28:4188.

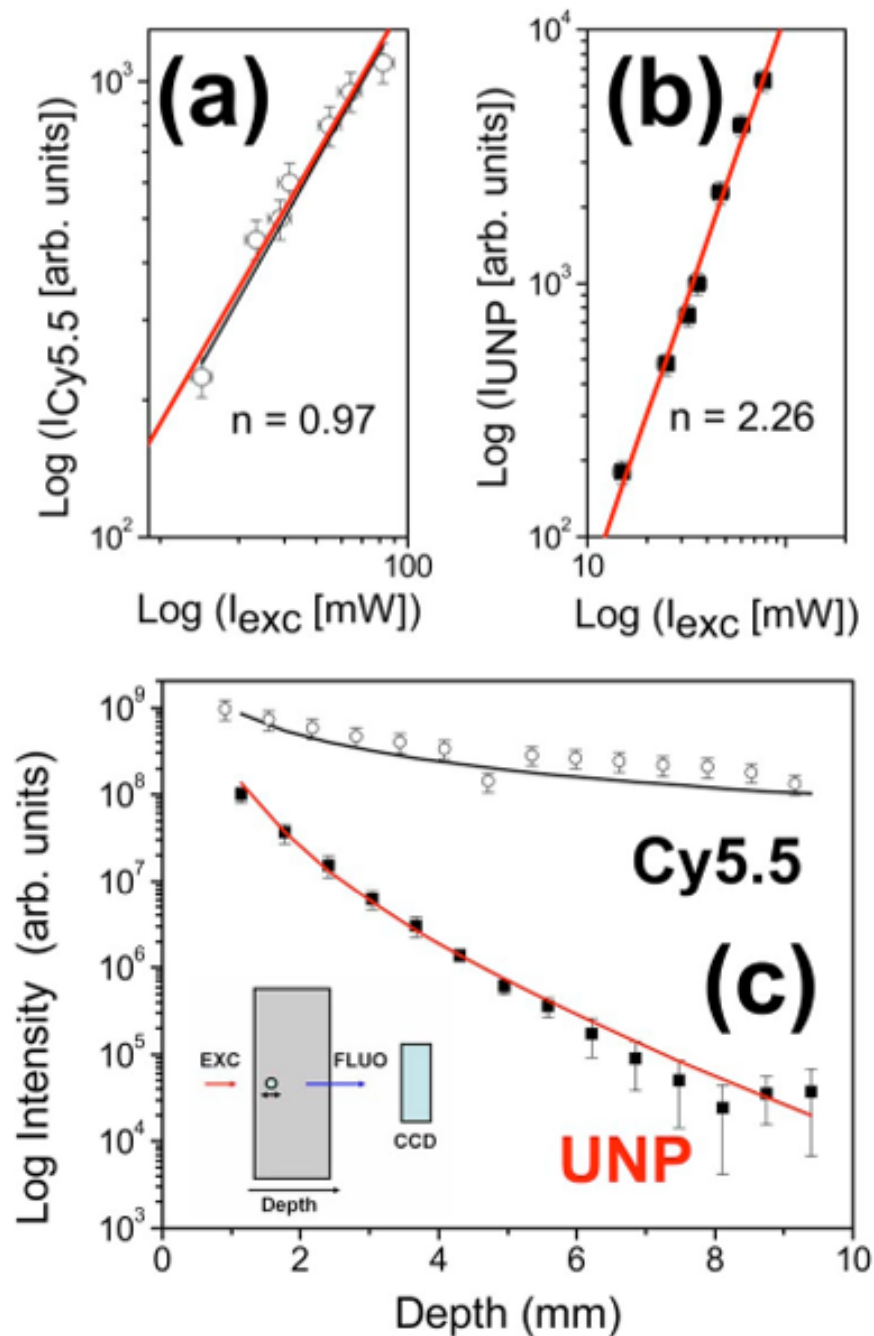


**Fig. 1.** (Color online) (a) Cy5.5 fluorescence signal as a function of the excitation power (open circles). Thick and thin lines represent the theoretical dependence and the best fit, respectively. (b) Upconverting nanoparticle fluorescence signal (squares). The line represents the best fit, demonstrating a nonlinear dependence (slope  $n=2.26$ ) of the fluorescence intensity on the excitation intensity. For the Cy5.5 fluorescence signal (linear dependence),  $n=0.97$ . (c) Intensity of the fluorescence signal at fixed excitation illumination for a 500  $\mu\text{m}$  diameter glass tube filled with a drop of Cy5.5 or UNP (top and bottom lines respectively). The signal is measured in transillumination mode as a function of depth within a chamber filled with an optically tissue-equivalent phantom that consists of intralipid and black India ink. Fluorescence detected at

710 nm after excitation at 680 nm for Cy5.5 (open circles) and upconverting fluorescence detected at 670 nm after excitation at 980 nm for UNP (filled squares) is plotted. Inset, the geometry of the experiment.

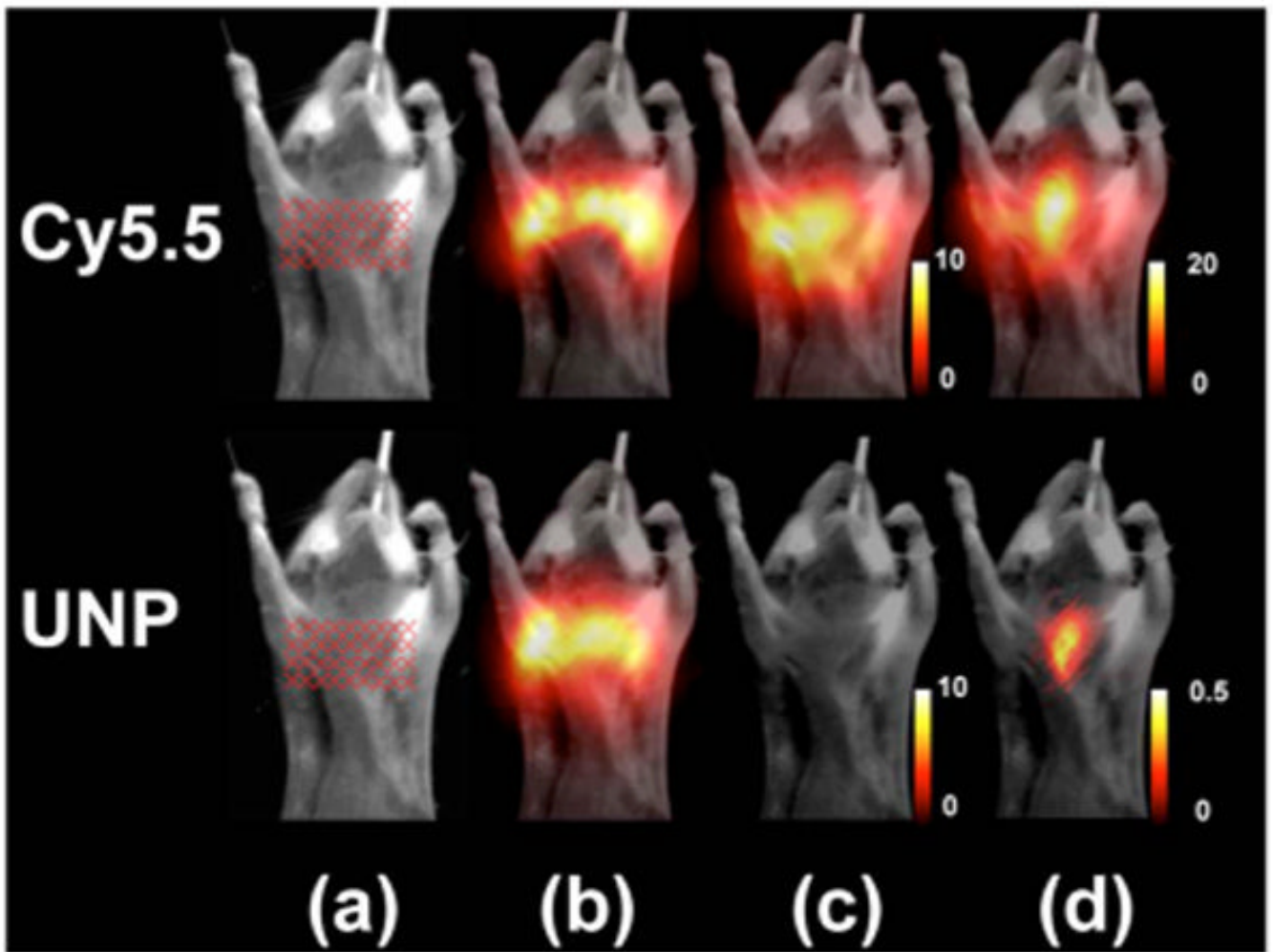


**Fig. 2.** (Color online) (a) White-light epi-illumination images of the mouse with a glass capillary tube inserted into the esophagus. The tube is filled with either Cy5.5 (upper row, excited at 680 nm) or upconverting nanoparticles (lower row, excited at 980 nm). Transillumination images averaged over all 36 sources are presented for (b) the intrinsic (c) the autofluorescence, and (d) the fluorescence signals. The transillumination signal is overlaid on top of the corresponding white image after color mapping.